

Reverse reaction magnetic field in two-wire high current busduct

Zygmunt Piątek, Dariusz Kusiak, Tomasz Szczegliński
 Czestochowa University of Technology
 42-200 Częstochowa, ul. Brzeźnicka 60a, e-mail: zygmunt.piatek@interia.pl,
 dariuszkusiak@wp.pl, szczegliński@interia.pl

Work has shown how a reverse reaction magnetic field influences the whole magnetic field within the conductor and its vicinity. A description of this is presented in formulae for relative field values and parameters taking into account frequency, conductivity and diameter of the conductor. This has shown the field to be an elliptical field.

1. Introduction

Unshielded double-wire high current busducts with tubular conductors (Fig. 1) can be installed in switching stations NN and WN [1-3].

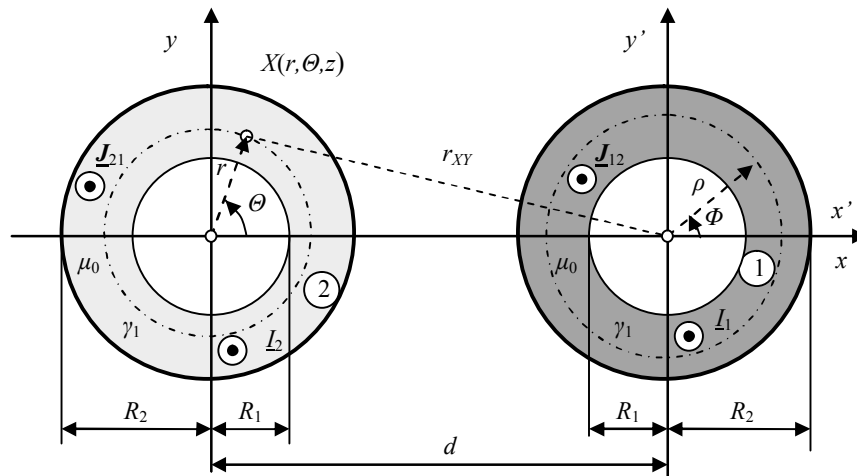


Fig. 1. Two-wire high-current busduct with the currents I_1 and I_2

Magnetic field $\underline{H}^w(r, \Theta)$ of current I_1 in the first tubular conductor induces on the second neighboring parallel tubular conductor eddy currents $\underline{J}_{21}(r, \Theta) = \mathbf{1}_z J_{21}(r, \Theta)$ (fig.1), which in external area generate reverse reaction magnetic field $\underline{H}^{rr}(r, \Theta)$ [4-6].

2. Magnetic field in the external area of the tubular conductor

Magnetic field $\underline{H}^{ext}(r, \Theta)$ in the external area ($r \geq R_2$) of the second tubular conductor

$$\underline{H}^{ext}(r, \Theta) = \underline{H}^w(r, \Theta) + \underline{H}^{rr}(r, \Theta) \quad (1)$$

where $\underline{H}^{rr}(r, \Theta)$ is the reverse reaction magnetic field outside of the conductor.

The electric field strength $\underline{E}^{rr}(r, \Theta)$, accompanying the magnetic field $\underline{H}^{rr}(r, \Theta)$ in the external area of the conductor ($r > R_2$), fulfills the scalar Laplace's equation

$$\nabla^2 \underline{E}^{rr}(r, \Theta) = 0 \quad (2)$$

whose solution, the separation of variables method, has the form

$$\underline{E}^{rr}(r, \Theta) = \sum_{n=1}^{\infty} \underline{E}_n^{rr}(r, \Theta) = \sum_{n=1}^{\infty} \underline{B}_n \frac{1}{r^n} \cos n\Theta \quad (2a)$$

where \underline{B}_n is a constant, which will be calculated from boundary conditions.

Applying the second Maxwell's equation to formula (2a), we obtain the complex form of the vector of the reverse reaction magnetic field strength outside the conductor

$$\underline{H}^{rr}(r, \Theta) = \mathbf{1}_r \underline{H}_r^{rr}(r, \Theta) + \mathbf{1}_\Theta \underline{H}_\Theta^{rr}(r, \Theta) \quad (3)$$

where

$$\underline{H}_r^{rr}(r, \Theta) = \sum_{n=1}^{\infty} \frac{n \underline{B}_n}{j\omega\mu_0 r^{n+1}} \sin n\Theta \quad (3a)$$

and

$$\underline{H}_\Theta^{rr}(r, \Theta) = -\sum_{n=1}^{\infty} \frac{n \underline{B}_n}{j\omega\mu_0 r^{n+1}} \cos n\Theta \quad (3b)$$

Constant \underline{B}_n is [7]

$$\underline{B}_n = \frac{j\omega\mu_0 \underline{I}_1}{2n\pi \underline{\Gamma}_1 R_1} R_2^n \left(\frac{R_2}{d}\right)^n \frac{\underline{s}_{cn}}{\underline{d}_{cn}} \quad (4)$$

where

$$\begin{aligned} \underline{s}_{cn} = & -n \beta_c K_n(\underline{\Gamma}_1 R_2) [I_{n-1}(\underline{\Gamma}_1 R_1) + I_{n+1}(\underline{\Gamma}_1 R_1)] + \\ & + n \{2 I_{n+1}(\underline{\Gamma}_1 R_2) K_n(\underline{\Gamma}_1 R_1) + I_n(\underline{\Gamma}_1 R_1) [K_{n-1}(\underline{\Gamma}_1 R_2) + K_{n+1}(\underline{\Gamma}_1 R_2)]\} + \\ & + \underline{\Gamma}_1 R_1 [I_{n+1}(\underline{\Gamma}_1 R_2) K_{n-1}(\underline{\Gamma}_1 R_1) - I_{n-1}(\underline{\Gamma}_1 R_1) K_{n+1}(\underline{\Gamma}_1 R_2)] \end{aligned} \quad (4a)$$

and

$$\underline{d}_{cn} = I_{n-1}(\underline{\Gamma}_1 R_2) K_{n+1}(\underline{\Gamma}_1 R_1) - I_{n+1}(\underline{\Gamma}_1 R_1) K_{n-1}(\underline{\Gamma}_1 R_2) \quad (4b)$$

where functions $I_n(\underline{\Gamma}_1 R_1)$, $K_n(\underline{\Gamma}_1 R_1)$, $K_n(\underline{\Gamma}_1 R_2)$, $I_{n-1}(\underline{\Gamma}_1 R_1)$, $K_{n-1}(\underline{\Gamma}_1 R_1)$, $I_{n-1}(\underline{\Gamma}_1 R_2)$, $K_{n-1}(\underline{\Gamma}_1 R_2)$, $I_{n+1}(\underline{\Gamma}_1 R_1)$, $K_{n+1}(\underline{\Gamma}_1 R_1)$, $I_{n+1}(\underline{\Gamma}_1 R_2)$ and $K_{n+1}(\underline{\Gamma}_1 R_2)$ are the modified Bessel's functions of the firsts and second kind respectively and of n , $n-1$ and $n+1$ order [8].

In the above formulas

$$\underline{\Gamma}_1 = \sqrt{j\omega\mu\gamma} = \sqrt{\omega\mu\gamma} \exp[j\frac{\pi}{4}] = k + jk = \sqrt{2j} k_1 \quad (5)$$

in which attenuation constant

$$k_1 = \sqrt{\frac{\omega_0\mu\gamma}{2}} = \frac{1}{\delta} \quad (5a)$$

where δ is the electrical skin depth, ω in an angular frequency, γ means electrical conductivity of conductor, and permeability of free space $\mu_0 = 4\pi 10^{-7} H \cdot m^{-1}$ [9-10].

Therefore the reverse reaction magnetic field in the external area of the second tubular busbar is determined by the formula (3), where its components, after replacing the \underline{B}_n constant, are

$$\underline{H}_r^{rr}(r, \Theta) = \frac{I_1}{2\pi \underline{\Gamma}_1 R_1 r} \sum_{n=1}^{\infty} \left(\frac{R_2}{r}\right)^n \left(\frac{R_2}{d}\right)^n \frac{\underline{s}_{cn}}{\underline{d}_{cn}} \sin n\Theta \quad (6)$$

and

$$\underline{H}_{\Theta}^{rr}(r, \Theta) = -\frac{I_1}{2\pi \underline{\Gamma}_1 R_1 r} \sum_{n=1}^{\infty} \left(\frac{R_2}{r}\right)^n \left(\frac{R_2}{d}\right)^n \frac{\underline{s}_{cn}}{\underline{d}_{cn}} \cos n\Theta \quad (6b)$$

If the above formulas refer to value

$$\underline{H}_0 = \frac{I_1}{2\pi R_2} \quad (7)$$

and following introduction of the relative distance between the conductors

$$\lambda_c = \frac{d}{R_2} \geq 1 \quad (8)$$

relative variable

$$\zeta = \frac{r}{R_2} \quad (9)$$

and parameter

$$\beta_c = \frac{R_1}{R_2} \text{ przy czym } (0 \leq \beta_c \leq 1) \quad (10)$$

Hence relative value components for the reverse reaction magnetic field are defined by the formulae

$$\underline{h}_r^{rr}(\zeta, \Theta) = \frac{1}{\sqrt{2j} \alpha_c \beta_c \zeta} \sum_{n=1}^{\infty} \left(\frac{1}{\zeta}\right)^n \left(\frac{1}{\lambda_c}\right)^n \frac{s_{cn}}{d_{cn}} \sin n\Theta \quad (11)$$

and

$$\underline{h}_{\Theta}^{rr}(\zeta, \Theta) = -\frac{1}{\sqrt{2j} \alpha_c \beta_c \zeta} \sum_{n=1}^{\infty} \left(\frac{1}{\zeta}\right)^n \left(\frac{1}{\lambda_c}\right)^n \frac{s_{cn}}{d_{cn}} \cos n\Theta \quad (11a)$$

where $\zeta \geq 1$ and $0 \leq \Theta \leq 2\pi$.

The distribution of the above components within the function of parameter α_c are presented in Figures 2 and 3.

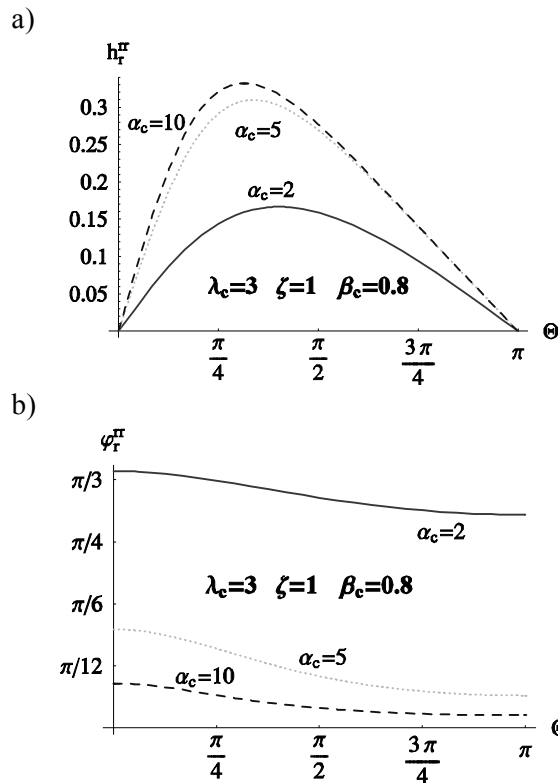


Fig. 2. The distribution of relative radial component values reverse reaction magnetic field:
a) the modulus, b) the argument

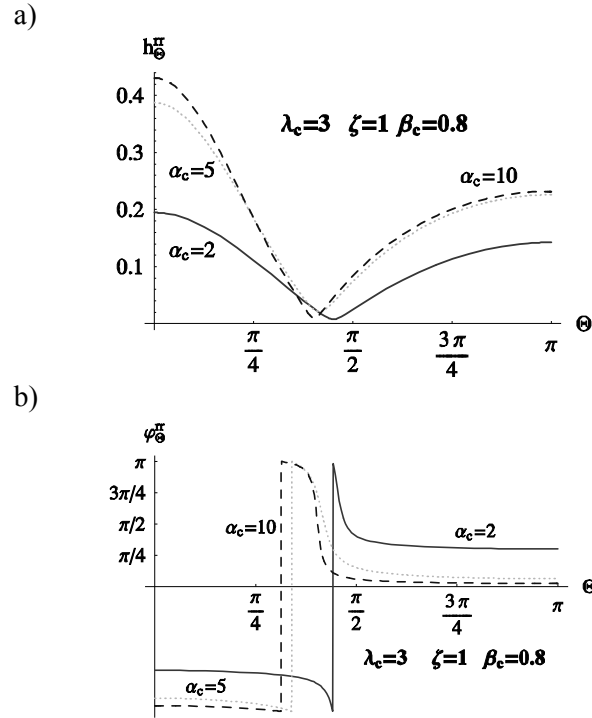


Fig. 3. The distribution of relative tangent component values reverse reaction magnetic field: a) the modulus, b) the argument

3. Distribution of the reverse reaction magnetic field modulus in external area

The set of arguments for the radial and tangential field components are different and therefore at each point the study area the reverse reaction magnetic field of the conductor is elliptic field. The relative value of this field modulus, relative value of the longer ellipsis semi axis expressed by the formula

$$h^{rr}(\zeta, \Theta) = h_1(\zeta, \Theta) + h_2(\zeta, \Theta) \quad (12)$$

where

$$h_1(\zeta, \Theta) = \frac{1}{2} \left| \underline{h}_r^{rr}(\zeta, \Theta) + j \underline{h}_\Theta^{rr}(\zeta, \Theta) \right| \quad (12a)$$

and

$$h_2(\zeta, \Theta) = \frac{1}{2} \left| \underline{h}_r^{rr*}(\zeta, \Theta) + j \underline{h}_\Theta^{rr*}(\zeta, \Theta) \right| \quad (12b)$$

The distribution of these values on the external surface of the second tubular busbar for various values of the α_c , parameter versus Θ angle is shown in Figure 4.

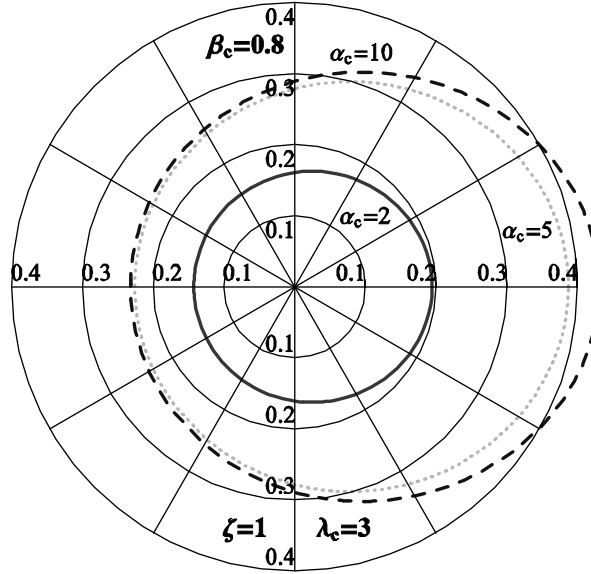


Fig. 4. The distribution of relative quantity the reverse reaction magnetic field modulus in the external area of the second busbar

For first conductor (fig. 1) the reverse reaction magnetic field has components

$$\underline{H}_r^{rr}(r, \Theta) = \frac{I_2}{2\pi \underline{\Gamma}_1 R_1 r} \sum_{n=1}^{\infty} (-1)^n \left(\frac{R_2}{r}\right)^n \left(\frac{R_2}{d}\right)^n \frac{s_{cn}}{d_{cn}} \sin n\Theta \quad (13)$$

and

$$\underline{H}_{\Theta}^{rr}(r, \Theta) = -\frac{I_2}{2\pi \underline{\Gamma}_1 R_1 r} \sum_{n=1}^{\infty} (-1)^n \left(\frac{R_2}{r}\right)^n \left(\frac{R_2}{d}\right)^n \frac{s_{cn}}{d_{cn}} \cos n\Theta \quad (13a)$$

Then, for relative values we have respectively

$$\underline{h}_r^{rr}(\zeta, \Theta) = \frac{1}{\sqrt{2j} \alpha_c \beta_c \zeta} \sum_{n=1}^{\infty} (-1)^n \left(\frac{1}{\zeta}\right)^n \left(\frac{1}{\lambda_c}\right)^n \frac{s_{cn}}{d_{cn}} \sin n\Theta \quad (14)$$

and

$$\underline{h}_{\Theta}^{rr}(\zeta, \Theta) = -\frac{1}{\sqrt{2j} \alpha_c \beta_c \zeta} \sum_{n=1}^{\infty} (-1)^n \left(\frac{1}{\zeta}\right)^n \left(\frac{1}{\lambda_c}\right)^n \frac{s_{cn}}{d_{cn}} \cos n\Theta \quad (14a)$$

The distribution of these values on the external surface of the first tubular busbar for various values of the α_c , parameter versus Θ angle is shown in Figure 5.

In the external area of the tubular busbar the magnetic field of reverse reaction is a field fading quickly, what is demonstrated in Figure. 6.

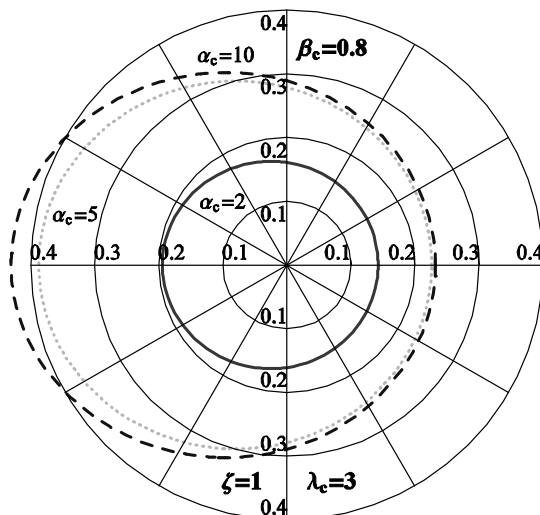


Fig. 5. The distribution of relative quantity the reverse reaction magnetic field modulus in the external area of the first busbar

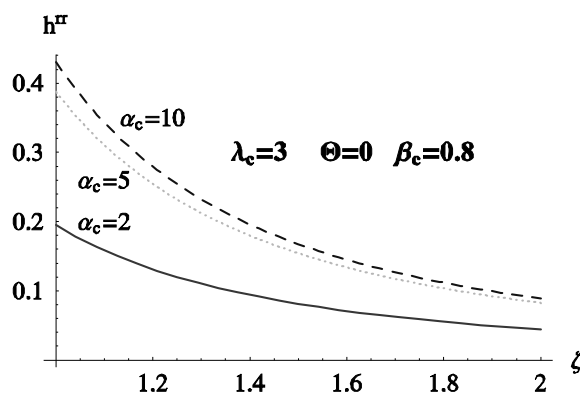


Fig. 6. The module of the magnetic field of reverse reaction within the tubular busbar external area

4. Conclusions

For a two-wire non-screened busducts the magnetic field distribution in busbars and in both internal and external area of tubular busbars is irregular, caused by the skin effect, but first of all by the proximity effect.

Figures 2 and 3 show, that the distribution of the magnetic field of reverse reaction in the external area of the busbar depends on the α_c parameter and is an irregular distribution with regard to the θ angle. Consequently, the total magnetic

field in the busbar and around it is irregular. Figures 4 and 5 show that the reverse reaction magnetic field assumes the highest values in the nearest point of the external source of the magnetic field.

The figures presented above show that the reverse reaction magnetic field, i.e. the external proximity effect and the skin effect should be taken into consideration when the magnetic field of high-current busducts is analysed, also for power frequency applications.

References

- [1] Piątek Z.: *Modeling of lines, cables and high-current busducts* (in Polish), Wyd. Pol. Częst., Częstochowa 2007.
- [2] CIGRE Brochure No 218.: *Gas Insulated Transmission Lines (GIL)*, WG 23/21/33-15, CIGRE, Paris, 2003.
- [3] Nawrowski R.: *High-current air or SF₆ insulated busducts* (in Polish), Wyd. Pol. Poznańskiej, Poznań 1998.
- [4] Piątek Z.: *Impedances of Tubular High Current Busducts*. Series Progress in High-Voltage technique, Vol. 28, Polish Academy of Sciences, Committee of Electrical Engineering, Wyd. Pol. Częst., Częstochowa 2008.
- [5] Baron B., Piątek Z.: Impedance and magnetic field of a tubular conductor of finite length (in Polish), *XXIII IC SPETO*, Gliwice-Ustroń 2000, ss. 477-484.
- [6] Piątek Z., Kusiak D., Szczegielniak T.: *Magnetic field of double-poles high current busduct* (in Polish), *Zesz. Nauk. Pol. Śl.* 2009, *Elektryka*, z.1(209), pp. 67-87.
- [7] Kusiak D.: *Magnetic field of two- and three-pole high current busducts*, Dissertation doctor (in Polish), Pol. Częst., Wyd. Elektryczny, Częstochowa 2008.
- [8] Mc Lachan N.W.: *Bessel functions for engineers* (in Polish), PWN, Warsaw 1964.
- [9] Piątek Z.: *Magnetic field in high-current isolated-phase enclosed bus ducts surroundings*, (in Polish), *Zesz. Nauk. Pol. Śl.* 1999, *Elektryka*, z. 166
- [10] Piątek Z., Kusiak D., Szczegielniak T.: *Magnetic field of the three phase flat high current busduct* (in Polish), *Zesz. Nauk. Pol. Śl.* 2009, *Elektryka*, z.1(209), pp. 51-65.